# Dual-Energy Computed Tomography and Beyond: Musculoskeletal System

Emtenen Meer, MBBS[a,b,*], Mitulkumar Patel, MD[a], Darren Chan, MBBS[a], Adnan M. Sheikh, MD[a], Savvas Nicolaou, FRCPC[a]

**KEYWORDS**

• Dual-energy CT • Musculoskeletal imaging • Gout • Collagen analysis

**KEY POINTS**

- Dual-energy computed tomography (DECT) detects bone marrow edema associated with occult fractures, osteolytic and non-osteolytic lesions in multiple myeloma, and osteomyelitis.
- In the assessment of arthropathies, DECT allows for quantification of monosodium urate deposition (gout), evaluation for pseudogout and utilization of iodine maps to detect psoriatic arthropathy.
- DECT overcomes numerous traditional limitations of conventional computed tomography offering clinical information previously seen only on MR imaging.
- DECT collagen applications have high accuracy in detecting ligamentous injuries in the knees, ankles, feet, and hands.
- DECT provides significantly improved image quality in metal artifact studies in musculoskeletal imaging.

## INTRODUCTION

Over the past decade, extensive research has been done to study dual-energy computed tomography (DECT), a tool that uses two different energy levels to provide material-specific information. Throughout recent years, DECT has proven to be an invaluable tool in radiology for its speed, reduced dose, and as an alternative to MR imaging in some instances.[1] This article discusses the novel techniques and applications that DECT has to offer in the MSK system, including the review of its most recent advances.

## BASIC PRINCIPLES AND TECHNICAL CONSIDERATIONS

The basic principle of DECT or spectral imaging is to be able to characterize different materials based on the relative absorption of x-rays at different energy levels. Usually, low (eg, 80 kVp) and high (eg, 140 kVp) x-ray tube voltages are used. For this to occur, tissue materials must be imaged simultaneously at the two energy levels. When the high and low x-ray energy spectra penetrate the tissues, Compton scatter and photoelectric effect are the two main types of interactions between photons and tissue matter. In computed tomography (CT), the attenuation of the photons mainly occurs due to the photoelectric effect, as its absorption is energy-dependent, making it critical for spectral tissue characterization.[2]

Different vendors and manufacturers achieve DECT imaging through various techniques (**Fig. 1**). A dual source with dual-detector array technique has less noise and lower risk of spatial and temporal misregistration compared with other techniques, with the downside of having a small second detector. The rapid kV-switching technique uses a single source which offers a high temporal resolution and an entire field of view but with slower acquisition time compared to dual-source CT and with the possibility of spectral overlap. Another technique is the single source

[a] Vancouver General Hospital-University of British Columbia, Vancouver, British Columbia, Canada; [b] King Faisal Specialist Hospital and Research Centre, Jeddah, Saudi Arabia
* Corresponding author. Vancouver General Hospital (VGH), 899 West 12th Avenue, Vancouver, BC V5Z 1M9.
*E-mail address:* Emtenan.meer@vch.ca

Radiol Clin N Am 61 (2023) 1097–1110
https://doi.org/10.1016/j.rcl.2023.05.008
0033-8389/23/© 2023 Elsevier Inc. All rights reserved.

Descargado para Anonymous User (n/a) en National Library of Health and Social Security de ClinicalKey.es por Elsevier en noviembre 17, 2023. Para uso personal exclusivamente. No se permiten otros usos sin autorización. Copyright ©2023. Elsevier Inc. Todos los derechos reservados.




**Fig. 1.** DECT imaging through various techniques compared to single energy CT. (*A*) Dual source DECT, (*B*) Rapid kV switching DECT, and (*C*) Single source with dual detectors DECT.

with a dual-detector layer which has the advantage of producing an entire field of view. The disadvantage of a single-source dual-detector technique is that it reduces soft tissue contrast and has a higher radiation dose.[3]

In DECT, postprocessing is vital, and various specific algorithms are used to reconstruct images for clinical interpretation. In practice, DECT can render material-specific and energy-specific images to be highly sensitive and specific aiding the interpreting radiologist. For example, when iodine is identified, iodine-only images can be created, and iodine can be color-coded, thus making it easy to tell apart from other dense materials such as acute blood. Another example of material-specific imaging is the virtual non-calcium (VNC), where voxels containing calcium can be excluded from the images, allowing for the identification of bone marrow edema (BME). In energy-specific imaging or virtual monoenergetic imaging, DECT can simulate conventional CT by providing images that display attenuation values similar to those expected when true monoenergetic x-ray beams are emitted. A single energy can be selected, either high or low, resulting in improved signal-to-noise and contrast-to-noise ratios, respectively.[4] Material-specific display aids in material differentiation and separation, whereas energy-specific display aids in material optimization. It is worth mentioning that although two energy levels and two sources are used in DECT, the dose is not increased compared with conventional CT, which is related to the fact that the administered radiation dose is divided between the two. Regarding time, the duration of image acquisition in DECT is similar to conventional CT; however, the radiologist may require more time to interpret the additional images provided by DECT based on the pathology of interest.

## ROLE IN SOFT TISSUE IMAGING

### *Gout*

Gout is an inflammatory disease characterized by monosodium urate (MSU) crystal deposition in the soft tissues and joints. Patients can present with an attack of acute gouty arthritis. Over time, repetitive attacks may result in chronic arthropathy with the development of tophi; soft-tissue masses that form secondary to chronic granulomatous reaction to MSU crystals. The diagnosis of gout is typically based on history, clinical examination, and serum urate; however, arthrocentesis is considered the most accurate method. However, arthrocentesis can be difficult and is not applicable in many cases, such as in small joints or joints that are difficult to access.[5,6] Arthrocentesis can also have several downsides and potential complications, such as an increased risk of infection and hematoma due to its invasive nature. Imaging the suspected joints and soft tissues with radiography, ultrasound (US), CT, and MR imaging aids in the initial evaluation,

Descargado para Anonymous User (n/a) en National Library of Health and Social Security de ClinicalKey.es por Elsevier en noviembre 17, 2023. Para uso personal exclusivamente. No se permiten otros usos sin autorización. Copyright ©2023. Elsevier Inc. Todos los derechos reservados.

differential diagnosis, and treatment follow-up with variable sensitivity and specificity.[7]

The emergence of DECT was a game changer for diagnosing gout and is now well recognized in the literature. By exploiting attenuation differences among variable materials, DECT can characterize MSU crystal deposits in the soft tissues. The reported sensitivity and specificity of DECT in gout detection are 90% to 100% and 83% to 89%, respectively.[8] With DECT gaining popularity and becoming increasingly available in many institutions, DECT serves as a less invasive alternative compared with arthrocentesis.[7]

Assessing for the presence of gout is achieved by using a two-material decomposition algorithm which will separate MSU crystals from calcium based on the atomic number. Then, MSU crystals can be color-coded, usually green, and overlaid on the grayscale images, which helps differentiate calcium from MSU deposits, and thus the diagnosis of gout can be made.[9] In addition to making the diagnosis, DECT has an excellent utility in mapping the distribution of the MSU crystals in the extremities.[10] In one study that looked at the distribution of MSU crystals using DECT, it was found that the first metatarsophalangeal (MTP) joint was the most involved, followed by the Achilles tendon, ankle joint, triceps tendon, and other MTPs, with less involvement of other assessed regions.[11]

DECT has the advantage of detecting gout in its early stages in patients who have normal urate levels. Furthermore, it can exclude the presence of gout in patients with hyperuricemia.[12] This is particularly useful in complex cases where DECT serves as a helpful diagnostic tool (**Fig. 2**). This has been demonstrated by a study by Nicolaou and colleagues, which reported five cases in which DECT was used to diagnose gout. In one case, DECT helped to rule out septic arthritis and malignant infiltration in a patient with chronic lymphocytic leukemia who had acute joint swelling and pain, making the diagnosis of gout, which was thought to be less likely.[13]

DECT can accurately quantify the amount of MSU deposits/tophi in patients with chronic gout using automated software. This allows for assessing the MSU deposits/tophi volume and disease burden before and after treatment, rendering it a valuable tool for follow-up.[12] The gout algorithm in DECT is not immune to artifacts. The most common artifact seen is the "nail bed artifact," which is thought to be related to similar dual-energy index values of the MSU crystal and the nail bed. Other less encountered artifacts include skin artifacts, submillimeter artifacts secondary to noise and scatter, and beam-hardening artifacts (**Fig. 3**).[14]

## *Pseudogout*

Pseudogout is another inflammatory arthropathy characterized by calcium pyrophosphate dehydrate (CPPD) crystal deposition in the articular and periarticular soft tissues. Diagnosis can be suggested when chondrocalcinosis is detected on radiography or CT. Arthrocentesis can also be used to make the diagnosis.[15] In inflammatory arthropathy, the presence of articular/periarticular mineralization in the absence of MSU crystal on DECT should raise the possibility of pseudogout.[16]

In pseudogout, DECT is useful for its ability to characterize the biochemical signature of the CPPD crystals and for its ability to quantify the crystal deposits.[17] The reported sensitivity of DECT to detect CPPD crystals is 77.8% compared with that of radiography 44.4%.[18] Although DECT is not ideal for early detection of calcium pyrophosphate crystals, it is thought to have a slightly better accuracy when compared with conventional CT

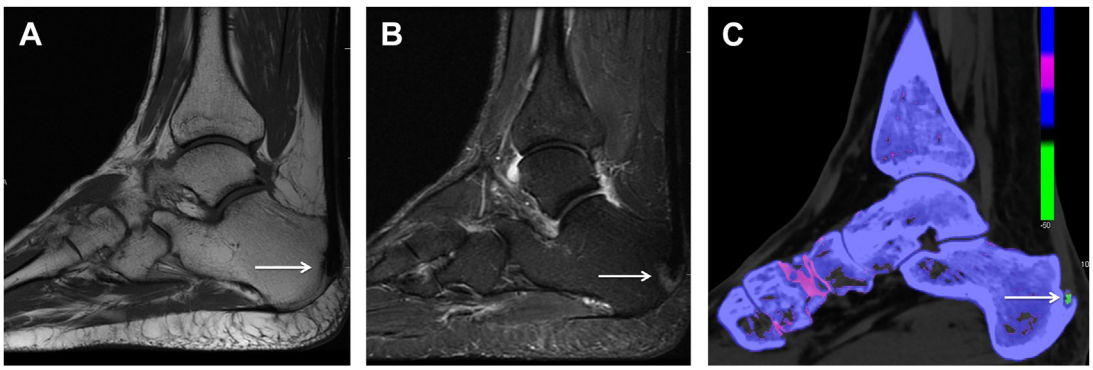



**Fig. 2.** DECT in a challenging case of gout. A 40-year-old man with left anterior ankle pain. Initial MR imaging was performed with (*A*) T1 and (*B*) PD fat saturated sequences showing low T1 and high PD signal intensity at the site of the Achilles attachment (*arrow*) suggestive of enthesitis. Four months later, (*C*) DECT showed a small amount of MSU deposits within the Achilles insertion (*arrow*).

Descargado para Anonymous User (n/a) en National Library of Health and Social Security de ClinicalKey.es por Elsevier en noviembre 17, 2023. Para uso personal exclusivamente. No se permiten otros usos sin autorización. Copyright ©2023. Elsevier Inc. Todos los derechos reservados.

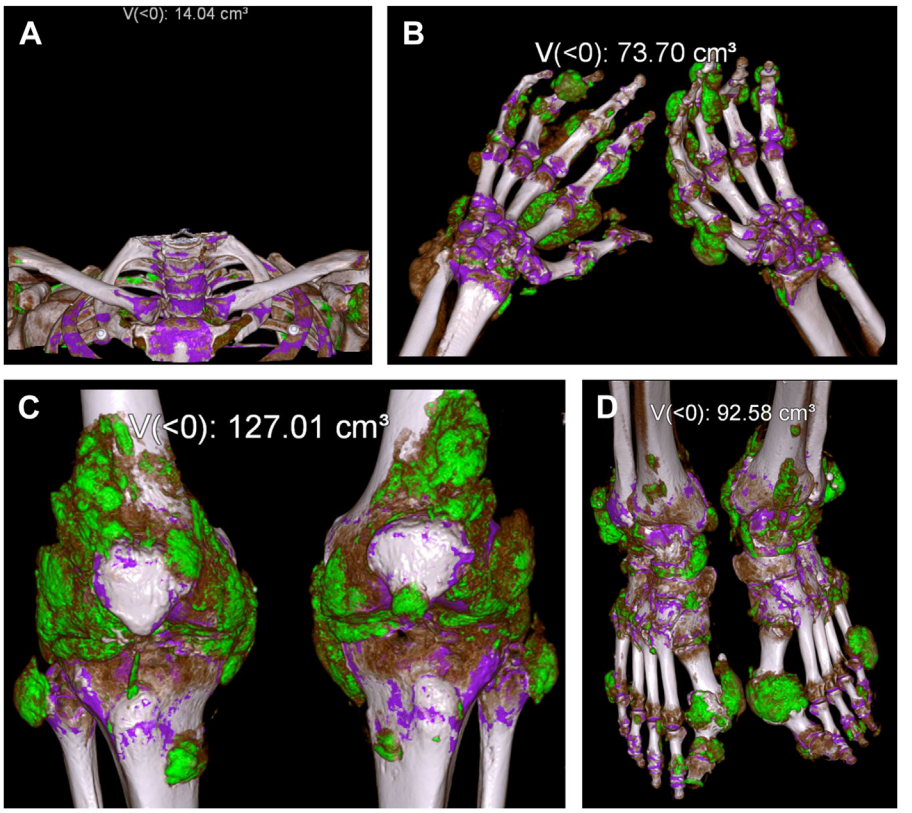



**Fig. 3.** Quantification and distribution of MSU deposits. A 54-year-old man with known gout. (*A*) 3D DECT images of the shoulders, (*B*) hands and wrists, (*C*) knees, and (*D*) ankles and feet show the exact distribution of the MSU deposits (color-coded *green*) in the joints as well as the MSU deposit burden per scanned region.

due to the color coding of the small structures on DECT[19,20] (**Fig. 4**).

Another benefit of DECT in the evaluation of pseudogout is collagen mapping. In the wrist, Ziegeler and colleagues studied collagen maps in patients with CPPD deposits. The study showed that DECT could detect tissue remodeling in the scapholunate (SL) ligament before the ligament eventually tears.

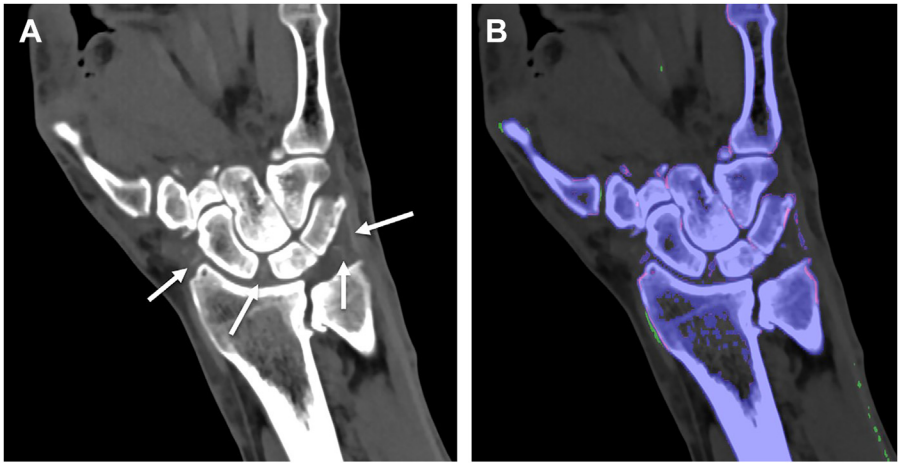



**Fig. 4.** Chondrocalcinosis in the knee. A 62-year-old patient with wrist injury. (*A*) Grayscale coronal image shows mineralization at the intercarpal joints and triangular fibrocartilage (*arrows*). (*B*) DECT in the same plane using the gout application shows blue foci corresponding to the mineralization, indicating chondrocalcinosis.

Descargado para Anonymous User (n/a) en National Library of Health and Social Security de ClinicalKey.es por Elsevier en noviembre 17, 2023. Para uso personal exclusivamente. No se permiten otros usos sin autorización. Copyright ©2023. Elsevier Inc. Todos los derechos reservados.

Their study shows that the SL ligament demonstrates high collagen density in patients with CPPD.[21] In the cervical spine, collagen mapping allows for the noninvasive quantification of CPPD in the atlantoaxial joint (AAJ). A recent study measured the mean densities of the AAJ ligaments in patients without inflammatory disease and showed that the mean collagen densities of the transverse ligament of the atlas, alar ligament, and nuchal ligament were 141.7, 117.3, and 110.6, respectively.[22]

### Psoriatic Arthritis

Psoriatic arthritis is an inflammatory arthritis that affects the joints and soft tissues, particularly the small joints of the hands. On imaging, radiographs, US, and contrast-enhanced MR imaging play a vital role in the diagnosis, prognostication, and management of psoriatic arthritis.[23] The utility of DECT using iodine mapping has been recently studied, and it was found that iodine maps are comparable to contrast-enhanced MR imaging in evaluating the inflammatory lesions seen in psoriasis. This is because CT has a superior spatial resolution, which becomes especially useful in assessing small joints.[24]

Iodine maps on DECT are also a valid tool for accurately evaluating the anatomical location of inflammation in psoriasis. The most common locations for involvement in the thumb, as depicted by DECT, include the sagittal band around the metacarpophalangeal joint, the medial collateral ligament of the interphalangeal joint, and the area surrounding the extensor pollicis longus tendon.[25] In addition, a DECT scoring system for the degree of psoriatic involvement in the joint has been recently created. This scoring system determines the presence of synovitis, flexor tenosynovitis, extensor peritendonitis, and periarticular inflammation. The degree of enhancement on iodine maps is subsequently assessed, and a score of 1 to 10 is given. The scoring system allows for quantitative assessment of the therapeutic response.[26]

### Collagen Analysis

Although MR imaging is considered the gold standard for assessing soft tissue injuries, MR imaging has the disadvantages of being time-consuming, expensive, and difficult to attain in an emergency setting compared with CT. On the other hand, conventional CT is not ideal for the assessment of soft tissue and ligaments. Over the past 2 decades, multiple papers have studied the utility of DECT in evaluating collagenous structures by using the tissue decomposition algorithm.[27,28] Studies have found that DECT is quick and readily available and has the added value of 3D rendering.[27]

In the knee, the anterior crucial ligament (ACL), posterior cruciate ligament (PCL), patellar, and quadriceps ligaments can be visualized on DECT.[27] Regarding the ACL, DECT was found to have a 93% accuracy rate for detecting both subacute and chronic complete ACL tears, with a sensitivity and specificity of 75% to 79% and 69% to 100%, respectively. In the acute setting, the presence of edema makes it difficult to clearly visualize the ACL.[1,29] For a higher accuracy assessment of the ACL, the knee should be looked at in the sagittal oblique plane with bone removal and soft tissue windowing.[30] In patients with knee ligament reconstruction, the collagen material decomposition application is a valuable tool for qualitative assessment of the reconstructed PCL, medial collateral ligament, lateral collateral ligament, anterolateral ligament, and medial patellofemoral ligament. However, the reconstructed ACL should be evaluated with caution on DECT.[31] Collagen analysis can also help in evaluating the meniscus in trauma cases and can show meniscal tearing, displacement, and herniation within a fracture pit (**Figs. 5** and **6**). In the ankle and foot, DECT was able to diagnose plantar plate tears, Achilles tendinopathy, and Achilles partial tears by using collagen material decomposition application which shows a decrease in collagen fibers at the site of injury.[11,32]

In the upper limb, DECT can show all the hand tendons allowing for accurate evaluation.[33] In addition, it can be used in the evaluation of ligamentous injury following penetrating trauma to the wrist, making it an MR imaging alternative for soft tissue assessment in the acute setting.[34] In the spine, the use of the VNC application with color coding has a higher diagnostic accuracy for the detection of lumbar disc herniation, the extent of disc displacement, and resultant spinal canal impingement compared with conventional CT. This makes DECT an appropriate alternative for MR imaging in claustrophobic patients and in centers where MR imaging is not readily available.[35,36]

### Other Soft Tissue Applications

Other less-studied DECT applications in the soft tissues of the MSK system have been reported. By exploiting the material decomposition of fat and soft tissues in the muscles, measurement of the muscle fat fraction can be achieved using DECT, enabling quantitative assessment of fatty degeneration in the rotator cuff.[37] Fat quantification on DECT is also a reliable tool for diagnosing and monitoring therapy in patients with sarcopenia[38] (**Fig. 7**).

Descargado para Anonymous User (n/a) en National Library of Health and Social Security de ClinicalKey.es por Elsevier en noviembre 17, 2023. Para uso personal exclusivamente. No se permiten otros usos sin autorización. Copyright ©2023. Elsevier Inc. Todos los derechos reservados.

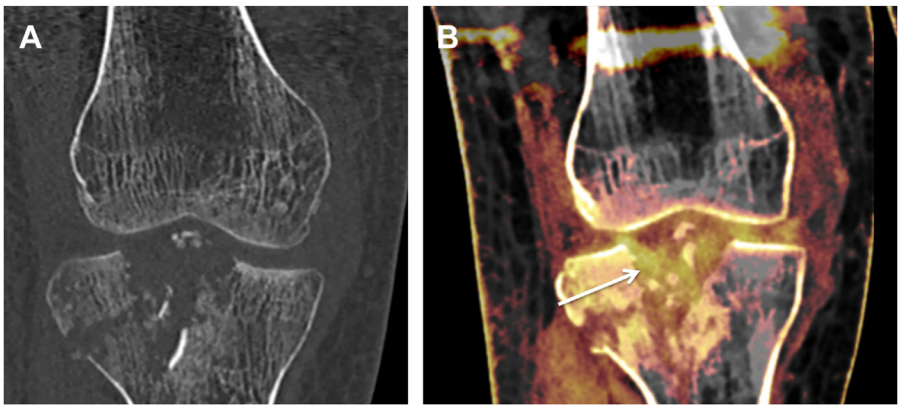



**Fig. 5.** Meniscal pathology on DECT. A 37-year-old patient who underwent a motor vehicle accident. Coronal images (*A*) show a tibial plateau fracture, and collagen analysis (*B*) shows herniation of the medial meniscus into the fracture cleft (*arrow*).

Pigmented villonodular synovitis or giant cell tenosynovitis is another pathology, in which DECT can aid in diagnosis. Spectral analysis with iron and calcium decomposition can help detect iron deposits in patients with knee or foot masses. The presence of iron deposits was found to correlate well with the "blooming" artifact seen on MR imaging.[39,40] DECT is also helpful in assessing soft tissue masses. A study predicts that spectral curves will be a promising tool for determining the benignity of lesions and found that an arc-shaped curve indicates the presence of abundant fat.[41] In addition, DECT is known to play a role in differentiating hyperdense blood products from calcification by using the VNC application, which becomes particularly useful in cases of trauma when patients present with a mass-like lesion.[4]

## ROLE IN BONE IMAGING

### *Occult Hip Fractures*

Conventional CT is a reasonable examination to perform in suspected occult hip fracture; however, the lack of cortical discontinuity or trabecular displacement can make it difficult for CT to delineate occult injuries and demonstrate their extent.[42] However, DECT visualization of BME may improve the depiction of subtle cortical or trabecular disruption by showing detail in areas that may otherwise be overlooked easily. DECT has been reported to have excellent accuracy in depicting occult proximal femoral fractures, with sensitivities ranging from 90% to 95%. However, the reported specificity varies among studies from as low as 40% to as high as 95%.[43,44]

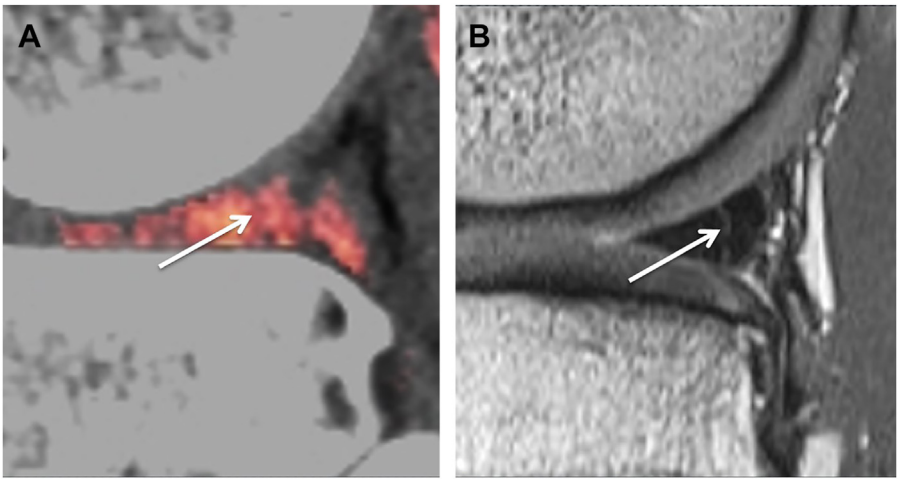



**Fig. 6.** Meniscal tear on DECT. A 48 year old with a twisting knee injury. (*A*) Color-coded DECT images show linear discontinuity at a cleft at the medial meniscus (*arrow*). (*B*) MR image shows a corresponding vertical tear (*arrow*).

Descargado para Anonymous User (n/a) en National Library of Health and Social Security de ClinicalKey.es por Elsevier en noviembre 17, 2023. Para uso personal exclusivamente. No se permiten otros usos sin autorización. Copyright ©2023. Elsevier Inc. Todos los derechos reservados.

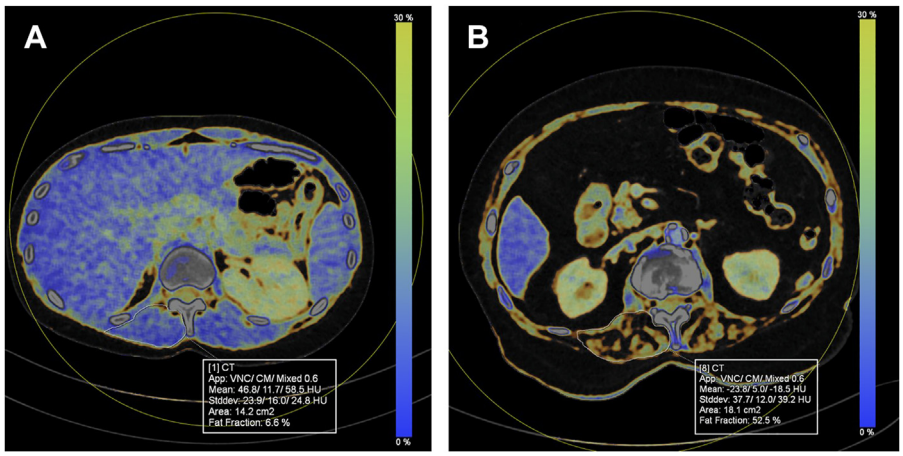



**Fig. 7.** Fat quantification on DECT. Fat mapping and fat friction calculations for the right paraspinal muscles at the level of L1 in two different patients. (*A*) A 30-year-old woman with a fat friction of 6.6%, compared with (*B*) a 92-year-old woman with multiple comorbidities and a fat friction of 52.5%.

An essential application of DECT in depicting proximal femoral fractures demonstrates the occult extension of a greater trochanter fracture into the intertrochanteric region.[45] A delayed diagnosis of intertrochanteric extension could lead to fracture displacement with the need for more extensive surgery, increased hospital stay, and delayed rehabilitation.[46] x-ray is the first line of investigation but has limited sensitivity to depict intertrochanteric extension, especially in osteopenia. MR imaging is the favored modality to show intertrochanteric extension, although it is often difficult to visualize the medial femoral cortex clearly.[47] DECT can aid in diagnosing intertrochanteric extension by demonstrating the extension of BME into this region, even in the absence of trabecular displacement, while allowing clear visualization of the cortical bone[42] (**Fig. 8**).

### *Osteoporotic Vertebral Compression Fractures*

When the axial load and bending forces surpass the inherent strength of the vertebra, it can lead to osteoporotic vertebral compression fractures.[42,48] If an early fracture goes undiagnosed, it can result in progressive vertebral collapse with the potential for extensive pain and disability.[42,49] Occult vertebral compression fractures may not be readily apparent at radiography or CT. MR imaging shows abnormal signal intensity at the fracture site, and a fracture line can sometimes be visualized.[42] DECT can show BME at the site of the occult vertebral body fracture similar to MR imaging (**Fig. 9**). Correlation with images obtained with the bone window setting may show subtle compression of a vertebral endplate or a cortical step-off. DECT can help differentiate a chronic fracture deformity without BME from an acute fracture with BME, just like MR imaging. DECT has shown excellent promise in helping identify osteoporotic vertebral compression fractures, with a sensitivity ranging from 85% to 90% and a specificity of over 95%.[42,50,51]

### *Periprosthetic Fracture*

Periprosthetic fractures occur in 4.1% of primary total hip arthroplasties. Delayed intervention could lead to poor outcomes with increased morbidity.[42,52] Although radiographs are the primary imaging modality to help assess periprosthetic fractures, subtle nondisplaced fracture lines around the components may be challenging to. MR imaging shows susceptibility artifacts due to the metallic implants, although titanium implants and metal artifact reduction (MAR) techniques can overcome this limitation. Conventional CT is also limited by beam hardening and streak artifacts from the prosthesis, but DECT can help identify subtle periprosthetic fractures by depicting BME in adjacent periprosthetic regions. It is essential to differentiate a periprosthetic fracture with an intact prosthesis (Vancouver type B1) from a fracture causing traumatic loosening (Vancouver type B2), as the former is treated with fixation alone. In contrast, traumatic loosening is usually treated with revision arthroplasty.[42,53]

### *Pathologic Fractures*

A pathologic fracture occurs when there is a fracture through a lesion, which may be a benign tumor, malignant neoplasm, or osteomyelitis.[42] The affected bone may be weakened by trabecular destruction caused by the lesion and upregulation

Descargado para Anonymous User (n/a) en National Library of Health and Social Security de ClinicalKey.es por Elsevier en noviembre 17, 2023. Para uso personal exclusivamente. No se permiten otros usos sin autorización. Copyright ©2023. Elsevier Inc. Todos los derechos reservados.

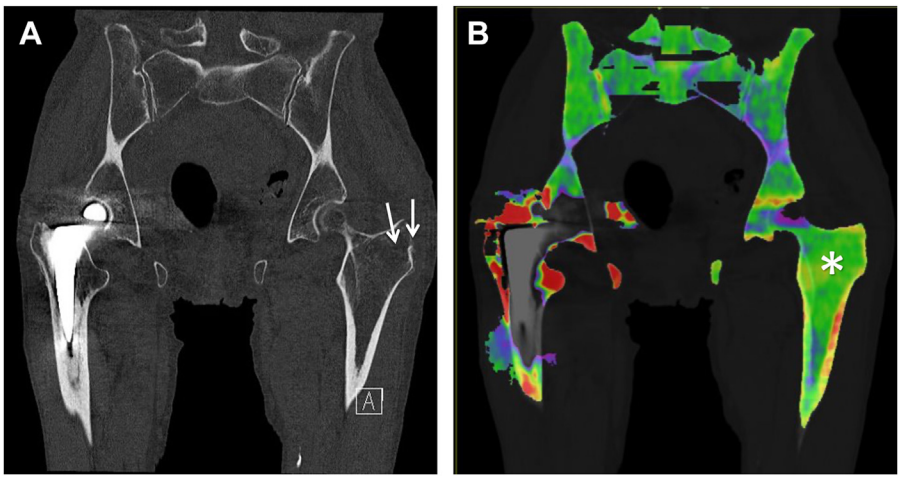



**Fig. 8.** DECT in occult hip fracture. A 73-year woman with a history of a fall. (*A*) Coronal CT pelvis shows non-displaced fracture of the left femoral greater trochanter (*arrows*). (*B*) DECT color map shows bone marrow edema extending through the intertrochanteric region (*asterisk*) with no definitive medial cortical breach identified on the grayscale image suggestive of intertrochanteric extension.

of osteoclast differentiation. Diagnosing pathologic fractures has long been challenging for radiologists, and MR imaging is the most common imaging examination performed to differentiate pathologic from non-pathologic fractures.[42,54] However, because MR imaging is not readily available in emergency settings, DECT can help characterize pathologic fractures. It can also depict BME associated with malignant lesions and help differentiate from the linear pattern of BME associated with a fracture (**Fig. 10**). One crucial potential pitfall of DECT is that acute hemorrhage into bones in a traumatic fracture may be falsely identified as a pathologic fracture. In the authors' experience, pathologic fractures show a relatively larger area of abnormality at DECT compared with the severity of the fracture. The absence of trabecular or cortical disruption at a focal point and contiguous involvement of the bone help differentiate metastatic bone involvement from simple fractures.[42]

## Multiple Myeloma

Plasma cell disorders pose a heterogeneous group of diseases with several patterns and degree of bone involvement. Multiple myeloma (MM) is a disorder characterized by uncontrolled clonal proliferation of malignant plasma cells, mainly in the bone marrow (BM).[55] It is the most frequent primary BM disorder in adults and causes around 1% of all neoplastic diseases. Bone involvement is the most persistent manifestation of MM and is responsible for a major part of morbidity and mortality associated with the disease.[55,56]

On imaging, x-rays, CT and MR imaging play a pivotal role in diagnosing the disease, prognosis,

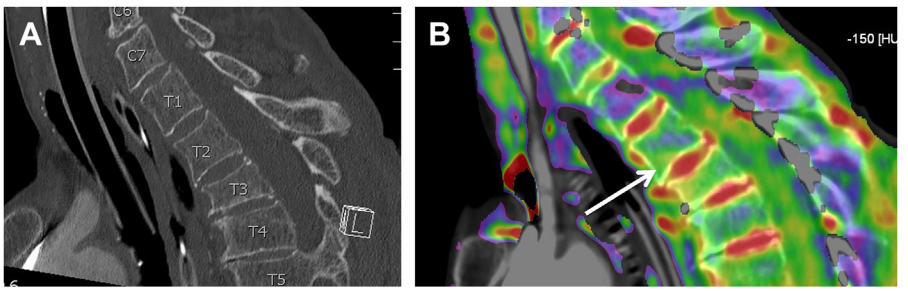



**Fig. 9.** DECT in osteoporotic vertebral fracture. An 83-year-old woman with a history of fall. (*A*) Sagittal CT image shows suspicious non-displaced fracture through anteroinferior T2 vertebral body with no significant loss of vertebral body height or bony retropulsion. There is also an acute wedge compression fracture of the body of T3 with 50% height loss. (*B*) DECT color maps show significant bone marrow edema in the anteroinferior T2 body (*arrow*).

Descargado para Anonymous User (n/a) en National Library of Health and Social Security de ClinicalKey.es por Elsevier en noviembre 17, 2023. Para uso personal exclusivamente. No se permiten otros usos sin autorización. Copyright ©2023. Elsevier Inc. Todos los derechos reservados.

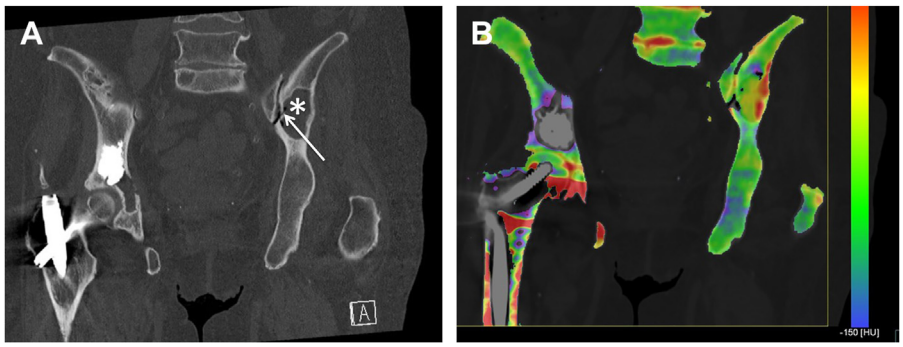



**Fig. 10.** Pathologic fracture on DECT. A 48-year-old woman with iliac bone metastatic lesion from thyroid cancer. (*A*) Coronal images show an iliac bone lytic lesion (*asterisk*) with a pathologic fracture (*arrow*) that extends into the sacroiliac joint with gas bubbles within the lesion and in sacroiliac bone. (*B*) DECT color maps demonstrate bone marrow edema relatively larger than the linear fracture area.

and management. The results of DECT using VNC are comparable to MR imaging in evaluating BM infiltration in MM (**Fig. 11**).[55] DECT can aid in detecting non-osteolytic BM infiltration of the spine and pelvis in patients with myeloma. BM infiltration can be qualitatively assessed using color-coded maps and quantitatively analyzed using Hounsfield unit measurements based on the region of interest (ROI). With MR imaging as a gold standard of reference, the use of the dual-energy VNC technique offers excellent diagnostic performance (sensitivity 93.3% and specificity 92.4% for the depiction of BM infiltration with an area under the receiver operating characteristic curve of 0.978 and a cutoff value of −44.9 HU).[55] Dual-energy VNC application may have a role in depicting non-osteolytic BM infiltration in MM. It can serve as a backup imaging modality for patients with contraindications for MR imaging and/or fluorodeoxyglucose PET/CT.[55]

## *Osteomyelitis*

The incidence of pyogenic osteomyelitis has recently increased, resulting in significant morbidity.[57,58] Imaging is usually required to determine the extent of tissue destruction in spondylodiscitis.[59] MR imaging accurately detects inflammatory BM lesions, destruction of the endplate and disc, and soft-tissue abscesses. Soft-tissue inflammation of the disc is the hallmark of the disease on imaging, that is, fluid-in-disc sign. Also, T1 typically reveals a loss of fat signal and a loss of endplate definition. The use of gadolinium further increases diagnostic accuracy with contrast-enhancement of inflammatory lesions. However, early imaging may be nonspecific for spondylodiscitis due to similarities with Modic I subchondral reactive edema.[57,60]

Although CT allows the detection of endplate destruction, it is not well suited for identifying soft-tissue involvement. Nevertheless, DECT visualizes

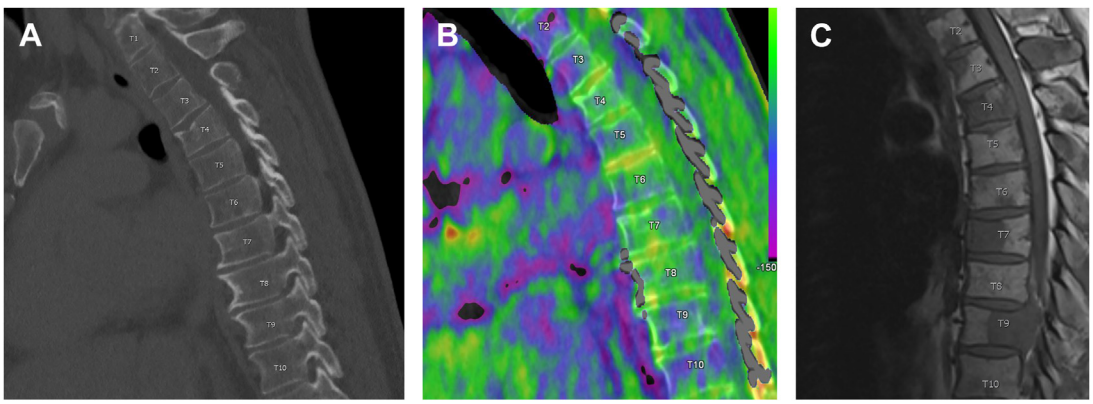



**Fig. 11.** DECT in multiple myeloma. A 36-year-old man with multiple myeloma (*A*) sagittal CT lumbar spine images are inconspicuous. (*B*) Color-coded dual-energy CT images show BM lesions comparable to (*C*) T1-weighted MR image.

Descargado para Anonymous User (n/a) en National Library of Health and Social Security de ClinicalKey.es por Elsevier en noviembre 17, 2023. Para uso personal exclusivamente. No se permiten otros usos sin autorización. Copyright ©2023. Elsevier Inc. Todos los derechos reservados.

connective tissue components by exploiting collagen's spectral properties.[2,57] DECT collagen mapping indicates severely altered connective tissue components with the destruction of the disc. Hence, DECT has added value compared with conventional CT for diagnosing spondylodiscitis, especially when MR imaging is unavailable or contraindicated, for example, in claustrophobia.[57,61]

### Role in Metal Artifact Reduction

An innovative application of the DECT is the MAR algorithm that functions through the implementation of the specific postprocessing for energy, which allows for creating a virtual monochromatic energy spectrum.[62,63] In cases with metallic implants, the metal artifacts reduce the diagnostic quality of conventional CT images. This limits the assessment of the implant integrity and evaluation of periprosthetic anatomical structures, increasing the risk of missing relevant findings.[62] The main mechanisms that create metal artifacts are photon starvation and beam hardening, scattering, partial volume effects, undersampling, and patient motion. DECT uses virtual monochromatic images (VMIs) by setting the different peak settings of kilovolts (photon energy) allowing users to freely select the optimal energy for maximum diagnostic image utility (usually between 40 and 140 keV).[62,64]

The hypothesis is that these monochromatic images are created once the data derived from higher (typically 140 kV) and lower beams (80–100 kV) have been processed. Moreover, the DECT workstation allows the image energy level to be adjusted to optimize the balance between soft tissue detail and artifact reduction. Compared with conventional CT, DECT demonstrates decreased susceptibility to beam-hardening artifacts, provides better quality, and enhances the visualization of the periprosthetic cortex, medullary bone trabeculation, and adjacent soft tissue (**Fig. 12**). These advantages are obtained without an increase in the total radiation dose.[65–67] Some studies have shown that the higher the energy levels of VMI, the greater the ability to reduce the effects of beam hardening. Bamberg and Zhou considered monochromatic energies with values between 95 and 150 keV to be more effective. They have also shown that the higher the energy values set, the more the tissue contrast is reduced.[62]

### Role in Computed Tomography Arthrography

Even though CT arthrography has been widely used in clinical practice since nearly the advent of CT, more research is still needed for optimization of this technique. The reported scan parameters differ by institution and radiologist, with most using a technique with 120 or 140 kVp tube energy and tube currents ranging from 125 to 200 mAs.[68] Subhas and colleagues performed a study attempting to optimize the single-energy CT arthrography technique and determine if DECT provides any additional benefit, specifically to identify and quantify iodine in cartilage. The result showed that iodine sensitivity (ie, change in attenuation per unit change in iodinated contrast concentration) increases as the tube voltage decreases, with 80 kVp having the highest sensitivity. The 80 kVp level was ~75% more sensitive to iodine than 120 kVp, ~50% more sensitive than linearly mixed DECT, and ~100% more sensitive than 140 kVp.[68] Usually, radiologists avoid using lower kVp, believing there will be more scatter and more noise. This is true if the tube current is kept constant; however, noise can be reduced if the tube current is increased. Likewise, although an increase in tube current can lead to an increase in dose when tube voltage is kept constant, the dose can be reduced by decreasing the tube voltage. Therefore, it is possible to deliver the same dose using different tube voltages by appropriately varying the tube currents.[68] The noise is nearly identical in the dose-matched single-energy CT techniques using different tube voltages and a dose-matched DECT technique. This allows us to select the optimal technique for the tissues being imaged, which is often cartilage in the case of CT arthrography. Subsequently, it was confirmed that the CT dose index (CTDI) values measured and calculated using a dosimeter matched very closely to the CTDI values displayed on the scanner. Hence, clinically, the CTDI values provided by the scanner can be used as a quick and easy method of comparing doses between techniques without the need to conduct dosimetry.[68–70]

DECT is a promising imaging modality for virtual unenhanced CT (VUCT) in single-contrast CT scanning. VUCT created from DECT has already been proven to have diagnostic value in abdominal and genitourinary imaging by identifying various lesions with fewer scans and lower radiation exposure.[71–73] Materials with a large atomic number, such as iodine, show higher attenuation on CT at low tube voltage settings. This characteristic is valuable when iodine needs to be differentiated from other materials, such as bone, renal stones, calcium plaques, hemorrhage, and instrumentation.[71,74] The HU ratio of a material at different tube voltages can be used to differentiate the composition of mixtures which can be achieved by DECT arthrography using this equation: mean HU at 80 kVp/mean HU at 140 kVp.[71]

Subhas and colleagues reported that the saturation of CT numbers (3071 HU) at 80 kVp occurs

Descargado para Anonymous User (n/a) en National Library of Health and Social Security de ClinicalKey.es por Elsevier en noviembre 17, 2023. Para uso personal exclusivamente. No se permiten otros usos sin autorización. Copyright ©2023. Elsevier Inc. Todos los derechos reservados.

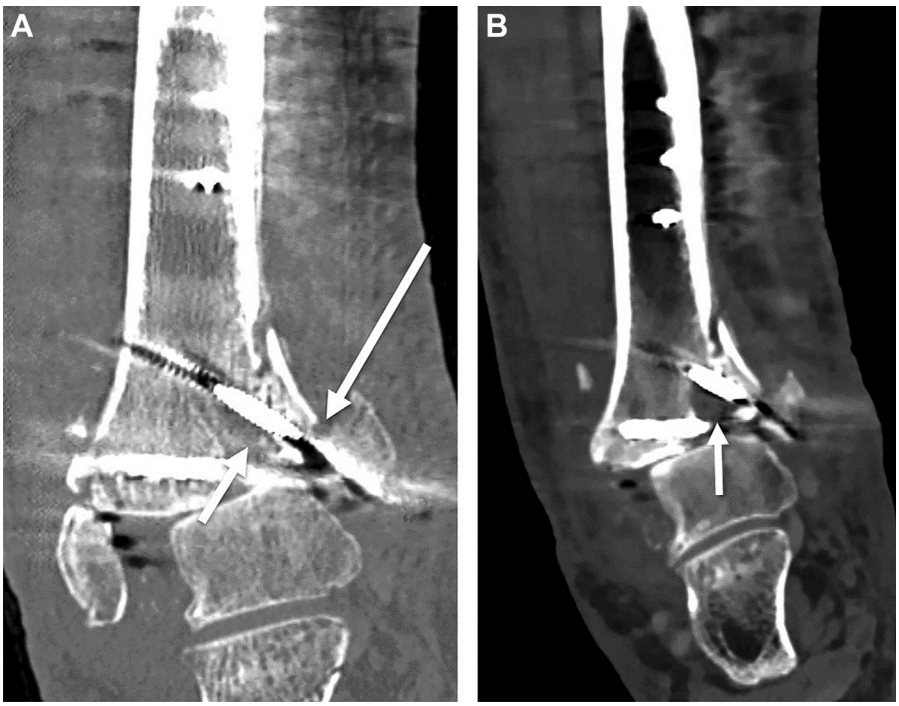



**Fig. 12.** Metal artifact reduction. A 50 year old with hardware failure with fracture. (*A*) Coronal CT of the leg shows the distal fibular metallic plate (*long arrow*), with possible loosening (*short arrow*). (*B*) Coronal CT in higher kV value better depicts the loosening around the plate (*short arrow*).

at 31% iodinated contrast material concentration and revealed that the saturation is limited by the lower 80 kVp saturation point, as with the DECT technique, which uses both 80 and 140 kVp.[71] The contrast material concentration higher than 31% could not be used in DECT arthrography for VUCT applications. Theoretically, the HU of iodine contrast mixture with a concentration over 30% should be 3071 on CT at 80 kVp. Moreover, the HU of contrast material at a concentration over 50% and 65% should be 3071 on CT at 120 and 140 kVp, respectively. However, when CT arthrography is performed in humans with a more concentrated iodinated contrast material, the HU shows variable values in a different ROI. The heterogeneity of HU is probably due to the heterogeneous mixing of synovial fluid and the contrast material or heterogeneous soft tissue content, such as synovium, in the selected ROI.[71]

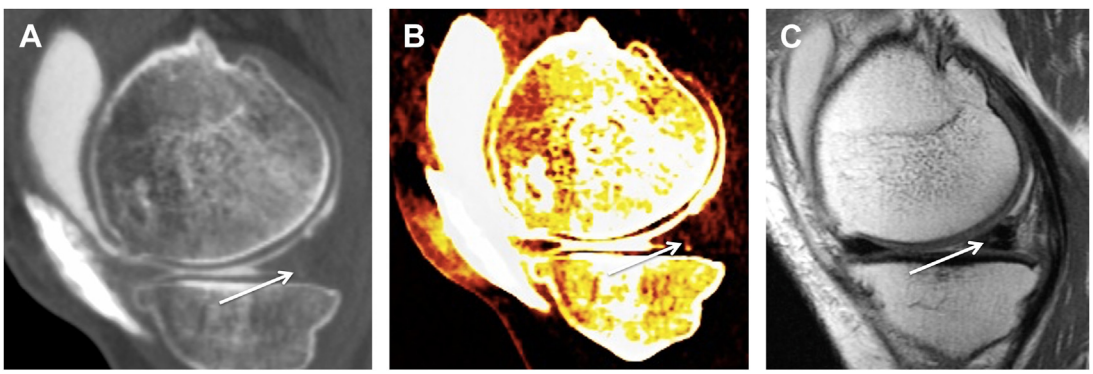



**Fig. 13.** DECT arthrography. A 43-year-old man with knee pain. (*A*) DECT arthrography shows iodinated contrast within the joint space with faint cleft of iodinated material extending into posterior horn of the meniscus (*arrow*). (*B*) Iodine map shows color-coded image with better delineation of the contrast material and meniscal tear (*arrow*). (*C*) MR image confirms the presence of small meniscal tear in the posterior horn (*arrow*).

Descargado para Anonymous User (n/a) en National Library of Health and Social Security de ClinicalKey.es por Elsevier en noviembre 17, 2023. Para uso personal exclusivamente. No se permiten otros usos sin autorización. Copyright ©2023. Elsevier Inc. Todos los derechos reservados.

DECT arthrography may be helpful for the preoperative diagnostic workup of intra-articular lesions and surgical planning regarding bone morphology (**Fig. 13**).[71]

## SUMMARY

In conclusion, DECT is a powerful and versatile imaging technique that has made significant advances in MSK imaging in recent years. Its ability to produce detailed images with comparable radiation to conventional CT makes it a valuable tool to every radiologist, especially as an alternative to MR imaging in the acute setting. The MSK system places significant value on DECT for imaging crystal arthropathy, identifying fractures, and minimizing metal artifacts. In the future, DECT is predicted to have a significant role in patients with psoriatic arthritis and in aiding the differential diagnosis of soft tissue masses. As this technology continues to improve and new techniques are developed, DECT will likely become an even more valuable tool for clinicians and patients.

## CLINICS CARE POINTS

- The gout application increases both the sensitivity and specifity for diagnosing gout on CT, and aids in the quantification of gout burden, in mapping MSU crystal distribution and in monitoring treatment response.
- Collagen analysis has a high accuracy for detecting soft tissue injuries when MRI is difficult to attain, however, in the acute setting, assessment may be limited due to the presence of soft tissue edema.
- The rate of detection of occult and microtrabicular fractures on CT improves by supplementing grey-scale CT images with virtual non-calcium application images.
- Metal artifact reduction algorithms can overcome the limitations produced by beam hardening artifacts produced by metallic hardware, and hence betters assessment for hardware integrity.

## DISCLOSURES

S. Nicolaou has a Master research agreement with Siemens Healthineers.

## REFERENCES


1. Fickert S, Niks M, Dinter DJ, et al. Assessment of the diagnostic value of dual-energy CT and MRI in the detection of iatrogenically induced injuries of anterior cruciate ligament in a porcine model. Skeletal Radiol 2012;42(3):411–7.
2. Nicolaou S, Liang T, Murphy DT, et al. Dual-energy CT: A promising new technique for assessment of the musculoskeletal system. Am J Roentgenol 2012;199(5_supplement). https://doi.org/10.2214/ajr.12.9117.
3. Mallinson PI, Coupal TM, McLaughlin PD, et al. Dual-energy CT for the musculoskeletal system. Radiology 2016;281(3):690–707.
4. Gibney B, Redmond CE, Byrne D, et al. A review of the applications of dual-energy CT in acute neuroimaging. Can Assoc Radiol J 2020;71(3):253–65.
5. Tashakkor AY, Wang JT, Tso D, et al. Dual-energy computed tomography: A VALID tool in the assessment of gout? Int J Clin Rheumatol 2012;7(1):73–9.
6. Kravchenko D, Karakostas P, Kuetting D, et al. The role of dual energy computed tomography in the differentiation of acute gout flares and acute calcium pyrophosphate crystal arthritis. Clin Rheumatol 2021;41(1):223–33.
7. Weaver JS, Vina ER, Munk PL, et al. Gouty Arthropathy: Review of clinical manifestations and treatment, with emphasis on imaging. J Clin Med 2021;11(1):166.
8. Wong WD, Shah S, Murray N, et al. Advanced musculoskeletal applications of dual-energy computed tomography. Radiol Clin 2018;56(4):587–600.
9. Chou H, Chin TY, Peh WC. Dual-energy CT in gout - A review of current concepts and applications. Journal of Medical Radiation Sciences 2017;64(1):41–51.
10. Sanghavi PS, Jankharia BG. Applications of dual energy CT in clinical practice: A pictorial essay. Indian J Radiol Imag 2019;29(03):289–98.
11. Mallinson PI, Stevens C, Reisinger C, et al. Achilles tendinopathy and partial tear diagnosis using dual-energy computed tomography collagen material decomposition application. J Comput Assist Tomogr 2013;37(3):475–7.
12. Desai MA, Peterson JJ, Garner HW, et al. Clinical utility of dual-energy CT for evaluation of Tophaceous Gout. Radiographics 2011;31(5):1365–75.
13. Nicolaou S, Yong-Hing CJ, Galea-Soler S, et al. Dual-energy CT as a potential new diagnostic tool in the management of gout in the acute setting. Am J Roentgenol 2010;194(4):1072–8.
14. Mallinson PI, Coupal T, Reisinger C, et al. Artifacts in dual-energy CT gout protocol: A review of 50 suspected cases with an artifact identification guide. Am J Roentgenol 2014;203(1). https://doi.org/10.2214/ajr.13.11396.
15. Rosenthal AK, Ryan LM. Nonpharmacologic and pharmacologic management of CPP Crystal Arthritis and BCP Arthropathy and periarticular syndromes. Rheum Dis Clin N Am 2014;40(2):343–56.
16. Rajiah P, Sundaram M, Subhas N. Dual-energy CT in musculoskeletal imaging: What is the role beyond gout? Am J Roentgenol 2019;213(3):493–505.


Descargado para Anonymous User (n/a) en National Library of Health and Social Security de ClinicalKey.es por Elsevier en noviembre 17, 2023. Para uso personal exclusivamente. No se permiten otros usos sin autorización. Copyright ©2023. Elsevier Inc. Todos los derechos reservados.

17. Pascart T, Norberciak L, Legrand J, et al. Dual-energy computed tomography in calcium pyrophosphate deposition: Initial clinical experience. Osteoarthritis Cartilage 2019;27(9):1309–14.
18. Tanikawa H, Ogawa R, Okuma K, et al. Detection of calcium pyrophosphate dihydrate crystals in knee meniscus by dual-energy computed tomography. J Orthop Surg Res 2018;13(1). https://doi.org/10.1186/s13018-018-0787-0.
19. Budzik JF, Marzin C, Legrand J, et al. Can dual-energy computed tomography be used to identify early calcium crystal deposition in the knees of patients with calcium pyrophosphate deposition? Arthritis Rheumatol 2021;73(4):687–92.
20. Tedeschi SK, Solomon DH, Yoshida K, et al. A prospective study of dual-energy CT scanning, US and X-ray in acute calcium pyrophosphate crystal arthritis. Rheumatology 2019;59(4):900–3.
21. Ziegeler K, Richter S-T, Hermann S, et al. Dual-energy CT collagen density mapping of wrist ligaments reveals tissue remodeling in CPPD patients: First results from a clinical cohort. Skeletal Radiol 2020;50(2):417–23.
22. Wittig TM, Ziegeler K, Kreutzinger V, et al. Dual-energy computed tomography collagen density mapping of the cranio-cervical ligaments—a retrospective feasibility study. Diagnostics 2022;12(12):2966.
23. Fassio A, Matzneller P, Idolazzi L. Recent advances in imaging for diagnosis, monitoring, and prognosis of psoriatic arthritis. Front Med 2020;7. https://doi.org/10.3389/fmed.2020.551684.
24. Fukuda T, Umezawa Y, Asahina A, et al. Dual Energy CT iodine map for delineating inflammation of inflammatory arthritis. Eur Radiol 2017;27(12):5034–40.
25. Ogiwara S, Fukuda T, Kawakami R, et al. Anatomical analysis of inflammation in hand psoriatic arthritis by dual-energy CT iodine map. European Journal of Radiology Open 2021;8:100383.
26. Kayama R, Fukuda T, Ogiwara S, et al. Quantitative analysis of therapeutic response in psoriatic arthritis of digital joints with dual-energy CT iodine maps. Sci Rep 2020;10(1). https://doi.org/10.1038/s41598-020-58235-9.
27. Sun C, Miao F, Wang X, et al. An initial qualitative study of dual-energy CT in the knee ligaments. Surg Radiol Anat 2008;30(5):443–7.
28. Alabsi H, Alreshoodi S, Low E, et al. Advancements in dual-energy CT applications for Musculoskeletal Imaging. Current Radiology Reports 2017;5(11). https://doi.org/10.1007/s40134-017-0249-1.
29. Peltola EK, Koskinen SK. Dual-energy computed tomography of cruciate ligament injuries in acute knee trauma. Skeletal Radiol 2015;44(9):1295–301.
30. Bai R, Li X, Li R, et al. Optimization of low-dose scan parameters in dual-energy computed tomography for displaying the anterior cruciate ligament. J Int Med Res 2020;48(7). https://doi.org/10.1177/0300060520927874. 030006052092787.
31. Jeon JY, Lee S-W, Jeong YM, et al. The utility of dual-energy CT collagen material decomposition technique for the visualization of tendon grafts after knee ligament reconstruction. Eur J Radiol 2019;116:225–30.
32. Stevens CJ, Murphy DT, Korzan JR, et al. Plantar plate tear diagnosis using dual-energy computed tomography collagen material decomposition application. J Comput Assist Tomogr 2013;37(3):478–80.
33. Deng K, Sun C, Liu C, et al. Initial experience with visualizing hand and foot tendons by dual-energy computed tomography. Clin Imag 2009;33(5):384–9.
34. Persson A, Jackowski C, Engström E, et al. Advances of dual source, dual-energy imaging in postmortem CT. Eur J Radiol 2008;68(3):446–55.
35. Booz C, Nöske J, Martin SS, et al. Virtual noncalcium dual-energy CT: Detection of Lumbar Disk Herniation in comparison with standard gray-scale CT. Radiology 2019;290(2):446–55.
36. Schömig F, Pumberger M, Palmowski Y, et al. Vertebral disk morphology of the lumbar spine: A retrospective analysis of collagen-sensitive mapping using dual-energy computed tomography. Skeletal Radiol 2020;50(7):1359–67.
37. Baillargeon AM, Baffour FI, Yu L, et al. Fat quantification of the rotator cuff musculature using dual-energy CT–a pilot study. Eur J Radiol 2020;130:109145.
38. Molwitz I, Leiderer M, McDonough R, et al. Skeletal muscle fat quantification by dual-energy computed tomography in comparison with 3T mr imaging. Eur Radiol 2021;31(10):7529–39.
39. Becce F, Federau C, Letovanec I, et al. Dual-energy computed tomography molecular imaging of pigmented villonodular synovitis. Rheumatology 2014;54(3):457.
40. Aggarwal A, Singbal SB, Yiew DS, et al. Pigmented villonodular synovitis. J Clin Rheumatol 2019;1. https://doi.org/10.1097/00124743-900000000-99087.
41. Sun X, Shao X, Chen H. The value of energy spectral CT in the differential diagnosis between benign and malignant soft tissue masses of the musculoskeletal system. Eur J Radiol 2015;84(6):1105–8.
42. Gosangi B, Mandell JC, Weaver MJ, et al. Bone marrow edema at dual-energy CT: A game changer in the emergency department. Radiographics 2020;40(3):859–74.
43. Reddy T, McLaughlin PD, Mallinson PI, et al. Detection of occult, undisplaced hip fractures with a dual-energy CT algorithm targeted to detection of bone marrow edema. Emerg Radiol 2014;22(1):25–9.
44. Kellock TT, Nicolaou S, Kim SS, et al. Detection of bone marrow edema in nondisplaced hip fractures:

Descargado para Anonymous User (n/a) en National Library of Health and Social Security de ClinicalKey.es por Elsevier en noviembre 17, 2023. Para uso personal exclusivamente. No se permiten otros usos sin autorización. Copyright ©2023. Elsevier Inc. Todos los derechos reservados.

Utility of a virtual noncalcium dual-energy CT application. Radiology 2017;284(3):798–805.
45. Kim SJ, Park BM, Yang KH, et al. Isolated fractures of the greater trochanter report of 6 cases. Yonsei Med J 1988;29(4):379.
46. Chana R, Noorani A, Ashwood N, et al. The role of MRI in the diagnosis of proximal femoral fractures in the elderly. Injury 2006;37(2):185–9.
47. Kim S-J, Ahn J, Kim HK, et al. Is magnetic resonance imaging necessary in isolated greater trochanter fracture? A systemic review and pooled analysis. BMC Muscoskel Disord 2015;16(1). https://doi.org/10.1186/s12891-015-0857-y.
48. Papaioannou A, Watts NB, Kendler DL, et al. Diagnosis and management of vertebral fractures in elderly adults. Am J Med 2002;113(3):220–8.
49. Kurtz S, Ong K, Lau E, et al. Projections of primary and revision hip and knee arthroplasty in the United States from 2005 to 2030. J Bone Joint Surg 2007;89(4):780–5.
50. Karaca L, Yuceler Z, Kantarci M, et al. The feasibility of dual-energy CT in differentiation of vertebral compression fractures. The British Journal of Radiology 2016;89(1057):20150300.
51. Kaup M, Wichmann JL, Scholtz J-E, et al. Dual-energy CT–based display of bone marrow edema in osteoporotic vertebral compression fractures: Impact on diagnostic accuracy of radiologists with varying levels of experience in correlation to Mr Imaging. Radiology 2016;280(2):510–9.
52. Griffiths EJ, Cash DJW, Kalra S, et al. Time to surgery and 30-day morbidity and mortality of periprosthetic hip fractures. Injury 2013;44(12):1949–52. https://doi.org/10.1016/j.injury.2013.03.008.
53. Marshall RA, Weaver MJ, Sodickson A, et al. Periprosthetic femoral fractures in the emergency department: What the Orthopedic Surgeon wants to know. Radiographics 2017;37(4):1202–17.
54. Fayad LM, Kamel IR, Kawamoto S, et al. Distinguishing stress fractures from pathologic fractures: A multimodality approach. Skeletal Radiol 2005;34(5):245–59.
55. Kosmala A, Weng AM, Heidemeier A, et al. Multiple Myeloma and Dual-Energy CT: Diagnostic Accuracy of Virtual Noncalcium Technique for Detection of Bone Marrow Infiltration of the Spine and Pelvis. Radiology 2018;286(1):205–13.
56. Dimopoulos M, Terpos E, Comenzo RL, et al. International Myeloma Working Group Consensus statement and guidelines regarding the current role of imaging techniques in the diagnosis and monitoring of multiple myeloma. Leukemia 2009;23(9):1545–56.
57. Eurorad.org. Eurorad. https://www.eurorad.org/case/16622. Accessed January 10, 2023.
58. Kehrer M, Pedersen C, Jensen TG, et al. Increasing incidence of pyogenic spondylodiscitis: A 14-year population-based study. J Infect 2014;68(4):313–20.
59. Esendagli-Yilmaz G, Uluoglu O. Pathologic basis of pyogenic, nonpyogenic, and other spondylitis and discitis. Neuroimaging Clin 2015;25(2):159–61.
60. Tali ET. Spinal infections. Eur J Radiol 2004;50(2):120–33.
61. Czuczman GJ, Marrero DE, Huang AJ, et al. Diagnostic yield of repeat CT-guided biopsy for suspected infectious spondylodiscitis. Skeletal Radiol 2018;47(10):1403–10.
62. Simonetti I, Verde F, Palumbo L, et al. Dual energy computed tomography evaluation of skeletal traumas. Eur J Radiol 2021;134:109456.
63. Aran S, Daftari Besheli L, Karcaaltincaba M, et al. Applications of dual-energy CT in emergency radiology. Am J Roentgenol 2014;202(4). https://doi.org/10.2214/ajr.13.11682.
64. Wellenberg RHH, Hakvoort ET, Slump CH, et al. Metal artifact reduction techniques in musculoskeletal CT-imaging. Eur J Radiol 2018;107:60–9.
65. Carotti M, Salaffi F, Beci G, et al. The application of dual-energy computed tomography in the diagnosis of musculoskeletal disorders: A review of current concepts and applications. La Radiologia Medica 2019;124(11):1175–83.
66. Lee YH, Park KK, Song H-T, et al. Metal artefact reduction in Gemstone Spectral Imaging dual-energy CT with and without metal artefact reduction software. Eur Radiol 2012;22(6):1331–40.
67. Bamberg F, Dierks A, Nikolaou K, et al. Metal artifact reduction by dual energy computed tomography using monoenergetic extrapolation. Eur Radiol 2011;21(7):1424–9.
68. Subhas N, Freire M, Primak AN, et al. CT arthrography: In vitro evaluation of single and dual energy for optimization of technique. Skeletal Radiol 2010;39(10):1025–31.
69. Reiser M, Karpf PM, Bernett P. Diagnosis of chondromalacia patellae using CT arthrography. Eur J Radiol 1982;2(3):181–6.
70. De Filippo M, Bertellini A, Pogliacomi F, et al. Multidetector computed tomography arthrography of the knee: Diagnostic accuracy and indications. Clin Imag 2009;33(6):493.
71. Chai JW, Choi J-A, Choi J-Y, et al. Visualization of joint and bone using dual-energy CT arthrography with contrast subtraction: In vitro feasibility study using porcine joints. Skeletal Radiol 2014;43(5):673–8.
72. Graser A, Johnson TR, Chandarana H, et al. Dual Energy CT: Preliminary observations and potential clinical applications in the abdomen. Eur Radiol 2008;19(1):13–23.
73. Fletcher JG, Takahashi N, Hartman R, et al. Dual-energy and dual-source CT: Is there a role in the abdomen and pelvis? Radiol Clin 2009;47(1):41–57.
74. Johnson TR, Krauß B, Sedlmair M, et al. Material differentiation by dual energy CT: Initial experience. Eur Radiol 2006;17(6):1510–7.

Descargado para Anonymous User (n/a) en National Library of Health and Social Security de ClinicalKey.es por Elsevier en noviembre 17, 2023. Para uso personal exclusivamente. No se permiten otros usos sin autorización. Copyright ©2023. Elsevier Inc. Todos los derechos reservados.